Carbohydrate Polymers 161 (2017) 90–98

Contents lists available at ScienceDirect

Carbohydrate Polymers

journal homepage: www.elsevier.com/locate/carbpol

Effect of β-glucan-fatty acid esters on microstructure and physical properties of wheat straw arabinoxylan films

Usman Ali[a,b], Vandana Bijalwan[a], Santanu Basu[b], Atul Kumar Kesarwani[a], Koushik Mazumder[a,*]

[a] National Agri-Food Biotechnology Institute, C-127 Industrial Area, Phase 8, SAS Nagar, Mohali, 160071, Punjab, India
[b] Dr. S. S. Bhatnagar University Institute of Chemical Engineering & Technology (SSBUICET), Panjab University, Chandigarh, India

ARTICLE INFO

Article history:
Received 5 September 2016
Received in revised form
13 December 2016
Accepted 17 December 2016
Available online 21 December 2016

Keywords:
Arabinoxylans
β-Glucan-fatty acid esters
Film microstructures
Water vapor permeability
Mechanical properties

ABSTRACT

Arabinoxylans (AX) was isolated from wheat straw, whereas β-glucan (BG) was extracted from oat flour. The compositional analysis indicated wheat straw AX contained arabinose and xylose as major constituent sugars whereas higher β-glucan content (77%) was found in the extracted material from oat flour. The BG was conjugated with lauric (LA), myristic (MA), palmitic (PA), stearic (SA) and oleic (OA) acid to prepare corresponding β-glucan-fatty acid esters (BGFAs) with nearly similar degree of substitution. The effect of BGFAs to AX films on the water barrier, optical and mechanical properties were investigated. The addition of LABG and MABG to AX formed laminar structures in the composite films which limited water vapor permeability, giving rise to more opacity. Films prepared by blending AX with SABG and OABG were less effective as water vapor barrier due to their non-layer film microstructures; however they were less opaque. The laminar structures also imparted less mechanical strength and flexibility in the composite films. Furthermore, thermogravimetric analysis (TGA) revealed that all AX-BGFAs composite films were thermally more stable than pure AX and AX-BG films.

1. Introduction

Agricultural crops residue are the cheep and abundant source of different valuable polysaccharides which are underutilized. Several value added product can be obtained from these agricultural crop residues. India is the second largest wheat producing country in the world after China. After the harvesting and threshing of the wheat, huge quantity of the crop residues such as wheat straw are either burnt or used for the animal feed. Wheat straw contains mainly cellulose (30–40%), hemicellulose (20–35%) and lignin (15–25%) (Ruiz et al., 2013). Hemicelluloses are heteropolysaccharides which consist both pentose and hexoses sugar residues. AX and arabino-glucuronoxylan (AGX) are the dominant hemicelluloses in the cell walls of lignified supporting tissues of grasses and cereals. They were isolated from sisal, corncobs and the straw from various wheat species (Ebringerova, Hromadkova, & Heinze, 2005). AX have a backbone composed of 1 → 4-linked β-D-xylopyranosyl (Xyl*p*) residues, which are often substituted at either on O-3 or O-2 (monosubstitution) or on both O-2 and O-3 (disubstitution) with arabinofuranose (Ara*f*) residues and to a much lesser extent with glucuronic acid residues (Ebringerova et al., 2005). In addition, phenolic acids have been found to be esterified to O-5 of some Ara*f* residues in AX. (1 → 3, 1 → 4) β-D-glucans commonly known as BG are hemicellulose components of cereal grains, where they are located in the sub-aleurone and endospermic cell walls (Ebringerova et al., 2005). Oat and barley usually contain around 3–5% BG, but some oat cultivars contain as much as 6–7% in the groat and some barleys even 12% or more (Ebringerova et al., 2005). β-D-glucans are linear homopolymers of D-glucopyranosyl (Glc*p*) residues linked mostly via two or three consecutive β-(1→ 4) linkages that are separated by a single β-(1 → 3) linkage (Ebringerova et al., 2005; Ying et al., 2015). Xylans have been studied for biodegradable film production, such as arabinoxylans from corn hulls and bran, rye flour, oat spelt, barley husks and wheat bran have been used in studies on film casting from aqueous solutions (Gröndahl & Gatenholm, 2007; Höije, Sternemalm, Heikkinen, Tenkanen, & Gatenholm, 2008; Mikkonen et al., 2009; Zhang & Whistler, 2004; Zhang et al., 2011). The excellent oxygen barrier properties and good mechanical properties of AX films have been demonstrated and their application as oxygen barriers in multilayer packaging has been suggested (Gröndahl & Gatenholm, 2007). Besides their well-documented health benefits and their wide use in the food industry due to their unique properties (Razzaq et al., 2016), β-glucans are also molecules of interest in different fields for

* Corresponding author.
E-mail addresses: koushik@nabi.res.in, kmazumder78@gmail.com (K. Mazumder).

http://dx.doi.org/10.1016/j.carbpol.2016.12.036
0144-8617/

their rheological, biocompatibility and biodegradability properties (Zhu, Du, & Xu, 2016). Furthermore, the film-forming ability of β-glucans have could be exploited to formulate new eco-sustainable edible coating material for food industry (Tejinder, 2003). Edible films from barley and oats β-glucans have been prepared (Tejinder, 2003). The films had good mechanical properties but poor moisture barrier properties than casein, gluten or arabinoxylan-based films (Mikkonen et al., 2009; Péroval, Debeaufort, Despré, & Voilley, 2002). Waxes have been investigated as hydrophobic component to improve moisture barrier properties of hydrophilic edible films; however these are being questioned due to their effect on human health by several organizations, causes development of undesired sensory properties and vegetarians may worry that coated food products contain animal based waxes (Arnon, Granit, Porat, & Poverenov, 2015; Jiménez, Fabra, Talens, & Chiralt, 2010). Different studies have reported the incorporation of fatty acids as lipid components in protein and polysaccharide based films to modulate the water vapor barrier properties such as addition of fatty acids to hydroxypropyl-methylcellulose (HPMC) (Jiménez et al., 2010), sodium caseinate (J. Fabra, Jiménez, Atarés, Talens, & Chiralt, 2009) and starch based films (Jimenez, Fabra, Talens, & Chiralt, 2012) have been described.

Our interest in this study was three fold. The isolation and compositional analysis of wheat straw AX and oat flour BG were naturally of interest. We were also interested in preparing fatty acid ester derivatives of BG and their characterization. Our third interest was in preparing composite films of β-D-glucan fatty acid esters with AX. In this account, we first describe the preparation of a series of hydrophobic saturated and un-saturated fatty acid β-D-glucan esters (BGFAs). BGFAs were further blended with wheat straw AX to improve the hydrophobic character of the composite films. Finally, a series of AX-BGFAs films were prepared and the effects of BGFAs on microstructure and functional properties (water barrier, mechanical, thermal and optical properties) of the AX based films were investigated. These edible or biodegradable films might be used to produce industrially useful coating material for food products.

2. Experimental

2.1. Materials

Authenticated varieties of wheat straw (HD-2967) and oat whole grain (Haryana Javi-8) were used for the extraction of polysaccharide. All the chemicals, enzymes and solvents were procured from Sigma-Aldrich chemicals (USA). Acetic anhydride was procured from Fisher scientific (India). GC column (DB-5) was procured from the Agilent Technologies (USA).

2.2. Extraction of BG

The extraction of the β-glucan (BG) from the whole oat grain was performed by acidic extraction method (Ahmad, Anjum, Zahoor, Nawaz, & Ahmed, 2010). Briefly, the whole oat grain was grinded in a commercial grinder and sieved to prepare oat flour. The oat flour was refluxed with 80% ethanol for 6 h, dried and further treated with 1 M NaOH at 45 °C, 90 min. The remaining impurities were removed by centrifugation; the supernatant was adjusted to pH 3.5 with citric acid and centrifuged. Finally, the supernatant was precipitated with 80% ethanol (1:2 v/v), centrifuged and lyophilized to prepare BG.

$$\text{Yield of BG (\%, W/W)} = (\text{weight of the dried BG/weight of the dried oat flour}) \times 100$$

2.3. Extraction of AX

Wheat straw was milled to prepare powder material and soaked overnight in chloroform and methanol (9:1) solution to remove lipophilic and colored materials. The resulting residue was further treated with 20% KOH containing 1% $NaBH_4$, overnight at room temperature (Gruppen, Hamer, & Voragen, 1992; Subba Rao & Muralikrishna, 2006). The alkali extracted material was centrifuged and supernatant was neutralized with glacial acetic acid. The neutralized extract was further dialyzed (6 × 5 l) and finally lyophilized to prepare wheat straw arabinoxylans (AX).

$$\text{Yield of AX (\%, W/W)} = (\text{weight of the dried AX/weight of the dried wheat straw powder}) \times 100$$

2.4. Composition of AX and BG

Carbohydrates content was determined by phenol sulfuric acid method (Dubois, Gilles, Hamilton, Rebers, & Smith, 1956). Briefly, 2 ml aliquot of AX and BG (50–500 μg/ml) were mixed with 1 ml of freshly prepared 5% aqueous solution of phenol. Subsequently, 5 ml of concentrated sulphuric acid was rapidly added into the mixtures and allowed to stand for 10 min, vortexed and placed in a water bath for 20 min at room temperature. The absorptions of the solutions were measured at 490 nm using spectrophotometer (UV-2700, Shimadzu, Japan). Standard solutions of xylose (50–500 μg/ml) for AX and glucose (50–500 μg/ml) for BG were used to construct calibration curves. The β-glucan was analyzed by method of McCleary and Codd (AOAC, 2000) using megazyme assay kit.

2.5. Neutral sugar composition analysis

The carbohydrate composition analysis of AX and BG were determined by preparing the alditol acetate derivatives (Fox, Morgan, & Gilbart, 1989). Briefly, AX and BG (~1–2 mg) samples were separately hydrolyzed with 2 M TFA at 120 °C for 2 h. The hydrolyzed material was further reduced with $NaBD_4$ (~20 mg) and acetylated with acetic anhydride and pyridine (1:1) at 80 °C, 20 min to prepare alditol acetate derivatives. Derivatized monosaccharides were analyzed with a GC instrument (Agilent Technologies 7890) coupled to a mass spectrometer. The sample (1 μl) was introduced in the split less injection mode in DB-5 (30 m × 0.25 mm, 0.25 μm film thickness, Agilent) using helium as carrier gas. The alditol acetate derivatives were separated using the following temperature gradient: 80 °C for 2 min, 80–170 °C at 30 °C/min, 170–240 °C at 4 °C/min, 240 °C held for 30 min and samples were ionized by electrons impact at 70 eV.

2.6. Total phenol measurement and estimation of uronic acid

The total phenolic (TP) content of AX was determined using Folin-Ciocalteu reagent as previously described (Singleton, Orthofer, & Lamuela-Raventos, 1998). TP was expressed as mg gallic acid equivalent (GAE) per gram of sample. The content of uronic acid in AX was estimated by carbazole method (Knutson & Jeanes, 1968).

2.7. Esterification of BG

Esterification of β-glucan was performed as previously described (Freire, Silvestre, Neto, & Rocha, 2005; Ratanakamnuan, Manorom, & Inthasai, 2013; Whistler, 1945). Briefly, 5 ml of fatty acid chloride and 2.5 ml of pyridine were added to BG sample (1 g) suspended in toluene. The reaction mixture was allowed to stand at 30°–80 °C for 5–24 h. After completion, the reaction mixture

was precipitated by ice-water (600 ml). The precipitated material was further purified by washing with ethanol, water and acetone respectively. The purified material was finally dried at room temperature to prepare BGFAs (LABG, MABG, PABG, SABG and OABG: lauric, myristic, palmitic, stearic and oleic acid-β-glucan esters).

2.8. Fourier transform infra-red (FTIR) analysis

The IR spectra of samples were recorded by Agilent Technologies, Cary 600 series spectrophotometer. The entire samples were analyzed by using the attenuated total reflectance method (Winkler, Vorwerg, & Wetzel, 2013); scans were collected in the frequency range of 500–4000 cm^{-1} at a resolution of 4 cm^{-1}.

2.9. Elementary analysis

Measurements were performed using the combustion technique on automatic elemental analyzer (FLASH 2000, Thermo Scientific) (Winkler et al., 2013; Vaca-Garcia, 2001). All the samples were analyzed in triplicates. The software ChemBioDraw Ultra 12.0 (Cambridge Soft) was used in the evaluation.

2.10. Film formation

2.10.1. Preparation of homogenous films

Homogeneous films were obtained after solubulization of AX and AX-BG (60:40, w/w) in ultrapure water under ultrasonic homogenization (Q700, QSonica LLC; USA) at a concentration of 20 g/l (Sárossy et al., 2013). Then, glycerol was added at concentration of 20% of total dry basis (Péroval et al., 2002; Phan The et al., 2002). The film forming solutions were spread into Teflon coated petri-dishes or plates. The films dried at 23 ± 1 °C with relative humidity of 50%

2.10.2. Preparation of AX-BGFAs films

Emulsion based films containing AX and BGFAs (60:40, w/w) were made according to the similar process used for homogeneous films except that addition of Tween-80 as emulsifier (3% of lipid phase) was done differently (Phan The et al., 2002). The film forming emulsions were spread and dried using the same technique that used for homogeneous films.

2.11. Droplet size

The volume distributions of the emulsion droplets were measured by dynamic light scattering (ZEN3600, Malvern instruments Ltd) (Otoni, Avena-Bustillos, Olsen, Bilbao-Sáinz, & McHugh, 2016). The film forming emulsions were placed in cuvette and analyzed at 25 °C. The average particle size value was recorded.

2.12. Film thickness

The thickness of the films was measured at 5–10 points using a micrometer screw gauge (Mitutoyo Corporation, Japan) with μm precession and an average film thickness was calculated (Sárossy et al., 2013).

2.13. Moisture content

Film pieces were equilibrated at 23 °C and three different relative humidifies (50% RH in climate chamber, 75% and 98% RH using a desiccator containing saturated solution of sodium chloride and potassium sulphate respectively (Höije et al., 2008). Moisture content of the film samples were measured by moisture analyzer (XM 60, Precisa) and the films were analyzed at 105 ± 1 °C until the equilibrium weight was obtained. All the films were analyzed in triplicate. The percentage of weight loss was determined using the following Eq. (1):

$$\text{Percentage moisture content} = F_2/F_1 \times 100 \quad (1)$$

Where F_1 and F_2 are the initial and final weight of the film

2.14. Scanning electron microscope (SEM)

The surface morphology of the films was characterized qualitatively by SEM (Rubilar et al., 2013). The films were maintained in vacuum desiccators with P_2O_5 for 2 days. Then, films were cut into small pieces, fixed on a holder and coated with gold. The microstructures of the films were examined with scanning electron microscope (JEOL JCM-6000 BENCHTOP, JEOL Ltd, Japan) with an accelerating voltage of 10 kV and magnification at 500 and 1500X.

2.15. Water vapor permeability (WVP)

Water vapor transmission rate (WVTR) of the films were determined by using the gravimetric method according to the ASTM E 96/E 96M-05 (ASTM, 2005), the cups were firstly filled with anhydrous calcium chloride leaving 5 mm space to the top. Circular films of nearly 20 mm diameter were placed over the mouth of test cups and sealed with vacuum silicone grease. Then, the assemblies were weighted and placed in a conditioned chamber at 22 ± 1 °C at 50 ± 1% RH. The cups were weighted every 2 h during first 12 h and then measurements were performed at interval of 24 h for 5 days until the stable weight was attained, the weight increment of cups were measured and plotted at intervals. The slope of the straight line was calculated as linear regression. The WVTR was determined using the Eq. (2).

$$\text{WVTR} = S/A \quad (2)$$

Where S and A correspond the slope of the weight gain against time curve (g/24 h) (Mukherjee & Ghosh, 2016) and exposed film area (m^2).

The water vapor permeability (WVP) was obtained by multiplying the WVTR by thickness of film and dividing it by water vapor partial pressure difference between the two sides of film.

2.16. Mechanical properties

Texture Analyzer (TA.XT plus, Stable microsystem) was used to determine the tensile strength (TS) and elongation at break (E%) of films according to the ASTM standard method 828-97 (ASTM, 2002). TS and E (%) were calculated from the stress-strain curves, estimated from force-distance data obtained from the different films (2 cm wide × 8 cm long), six replicates were analyzed for each formulation of film. Before testing, films were equilibrated for one week at 58% RH. Equilibrated films were mounted in film-extension grips with an initial grip separation of 50 mm and stretched at 0.5 mm/s crosshead speed until breaking. The TS and E (%) was expressed in MPa and were calculated according to Eqs. (3) and (4):

$$TS = (F/A) \quad (3)$$

$$E\% = (l - l_1)/l_1 \times 100 \quad (4)$$

Where F is the maximum force for breaking films, A is the cross sectional area of films (thickness × width), l_1 is the initial length of film and l is the length of film at breaking point.

2.17. Optical properties

A spectro-colorimeter (Color Flex EZ, Hunter Lab, USA) was used to obtain infinite reflectance spectra of films. The measurements

were determined from 500 to 700 nm on both white and black background. Internal transmittances (Ti) of films were determined by applying the Kubelka-Munk theory for multiple sacctering to reflection spectra (Hutchings, 1999).

L*, a* and b* values of the films from CIE LAB color space were determined using a D_{65} illuminant and 10° standard observer. The whiteness (WI) indexes the films were determined using Eq. (5).

$$WI = \sqrt{100\text{-}(100\text{-}L*)^2 + a*^2 + b*^2} \quad (5)$$

Where L* (black 0 to white100), a*(red 120 to green −120) and b* values (yellow 120 to blue −120) values correspond to whiteness, redness and yellowness respectively.

2.18. Thermogravimetric analysis (TGA)

TGA analysis was performed with a Mettler Toledo thermogravimetric analyzer (Switzerland). Samples of ~5–10 mg were placed in a platinum crucible and heated in the TGA furnace; the measurements were carried out under nitrogen atmosphere with a heating rate of 10 °C from 30 to 650 °C (Mohajer, Rezaei, & Hosseini, 2016). Weight losses of samples were measured as a function of temperature. For a verification of results, all samples were measured twice. As a reliable deviation for the given temperatures, ±1 °C was the average result.

2.19. Statistics

The measurements of yield, composition, average particle size, water content, WVP, mechanical and optical properties were performed in triplicate. Data were expressed as mean ±SD and analyzed using the Graph Pad 6.0 software. Analyses of variance were performed by ANOVA procedure (Dunnett and Tukey's method, $P < 0.05$).

3. Result and discussion

3.1. Isolation and compositional analysis of AX and BG

The yield and composition of AX and BG materials were given in Table 1. AX was isolated from wheat straw with a yield of 17.3 (±1.1) whereas 10.3% (±0.9) yield of BG was obtained from oat bran. The compositional analysis of AX showed the presence of arabinose and xylose as major neutral sugar constituents (Supplementary Fig. S1) whereas the higher uronic acid content (9.4%) could be due to acidic arabinoxylans known to occur in cell walls of grasses and cereals (Ebringerova et al., 2005). The compositional analysis of oat bran BG contained glucose (80.7%) as major constituent whereas presence of some arabinose (3.6%) and xylose (15.7%) suggested co-extraction of arabinoxylans (Supplementary Fig. S1). The purity of β-glucan (77%) was comparable to previously reported values (Sárossy et al., 2013). The total phenolic content in AX was 23.4 mg of GAE/g of sample.

3.2. Esterification of BG and FTIR analysis

β-glucan was esterified by the fatty acid chloride-pyridine mixture and FTIR spectra were collected for the structural characterization of BGFAs (Fig. 1). The presence of polysaccharides in the sample was confirmed by occurrence of absorption band in the range of 1000–1200 cm^{-1} (Ahmad et al., 2010). The BGFAs showed an absorption band at 898 cm^{-1} correspond to the β-(1 → 4) linkages. The characteristic broad and intense bands and shoulder in the range 1031–1093 and 1159 cm^{-1} also suggested the stretching of (C—C) and (C—O) groups due to presence of glucopyranose and linear structure of β-glucan linked through (1 → 3) linkage (Ahmad et al., 2010). A sharp stretching peak in the region of 1740 cm^{-1} suggested the presence of C=O group of carboxyl ester moiety of esterified fatty acids. The bands in the region of 2854–2920 cm^{-1} were ascribed to C—H vibrations, mainly of fatty acids and glucose residues. The broad absorption band in the range 1374–1461 cm^{-1} was due to bending of C—H group (Xu, Miladinov, & Hanna, 2004).

Furthermore, no significant variations were observed in the relative ratios of height of ester band and height of β-glucan band, suggesting all BGFAs had nearly similar degree of fatty acid substitution (DS). The absolute DS values from elementary analysis were in the range of 2.03-2.17 which was in agreement with the FTIR data (Winkler et al., 2013). The detail of IR band ratios and elementary analysis was shown in Table 2.

Table 1
Yield and composition of AX and BG.

Sample type	AX	BG
Yield (%)	17.3 ± 1.1	10.3 ± 0.9
Carbohydrate content (%)	87.8 ± 3.5	88.2 ± 3.6
Neutral sugar composition (mole%)		
Xyl	78.5 ± 1.9	15.7 ± 0.9
Ara	13.6 ± 1.1	3.6 ± 0.4
Man	6.1 ± 0.2	nd
Gal	1.8 ± 0.5	nd
Glc	nd	80.7 ± 4.3
UA (wt%)	9.4 ± 0.8	–
β-glucan content (%)	–	77 ± 1.2
TP (mg GAE/g sample)	23.4 ± 2.6	

Ara: arabinose, Xyl: xylose, Man: mannose, Gal: galactose, Glc: glucose, UA: uronic acid, nd: not detected.

3.3. Lipid particle size

The study related to lipid particle size and distribution of film forming emulsion is important due to its impact on the film microstructure and physical properties. Table 2 represents the mean particle size of the film forming emulsion containing AX and BGFAs which showed the mean particle diameters were bigger for emulsion containing saturated fatty acids than those with unsaturated OA. The results suggested that decrease in polarity and increase in the chain length of fatty acids from LA to SA-BGs were associated with high degree of aggregation of saturated fatty acids in the film forming emulsion and facilitated the increase in average particle size and width of distribution (Fabra et al., 2009). In this sense, the largest fatty acid containing AX-SABG produced biggest particle size (2.048 μm) whereas smallest particle size (0.640 μm) was observed for AX-LABG. On contrary, the greater hydrophilic nature of unsaturated OABG facilitated the polar interactions with AX, thus increased the ease of dispersion (Jiménez et al., 2010). Furthermore, the greater polarity of OA might be responsible for low critical micelle concentration and smaller lipid aggregates (Jiménez et al., 2010).

3.4. Film forming and material properties

In our study, AX was blended with BG or BGFAs in the ratios of 60:40 (w/w) as previous studies revealed that addition of BG in nearly equal proportion to AX based films improved the tensile strength (Sárossy et al., 2013; Ying et al., 2015). All the cast films were brittle without addition of plasticizer (glycerol) whereas emulsifier (Tween-80) was added to stabilize the film structures during film drying and improved moisture barrier properties (Péroval et al., 2002; Phan The et al., 2002; Phan The, Debeaufort, Voilley, & Luu, 2009). Previous studies on oat spelt arabinoxylan and maize bran arabinoxylan-lipid based films recommended addition of glycerol as plasticizer for cohesive film formation (Mikkonen et al., 2009; Péroval et al., 2002). Similar studies on starch and

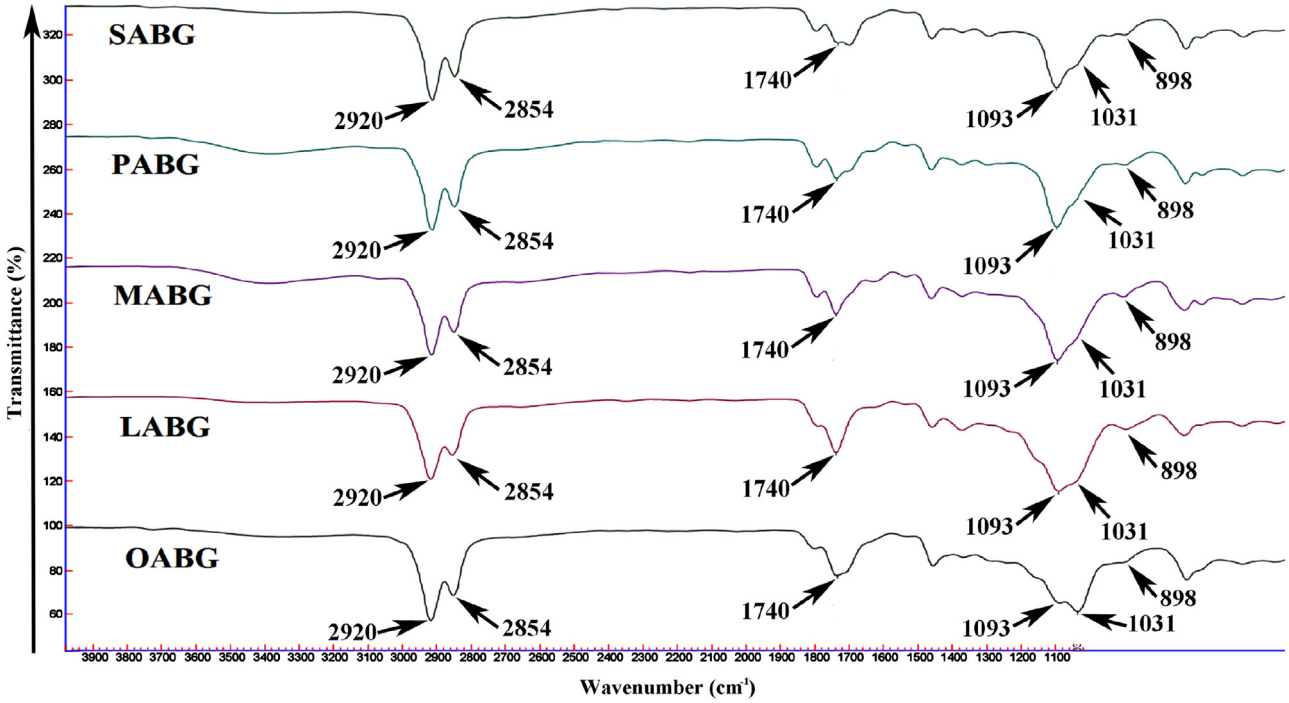

Fig. 1. ATR-FTIR spectrum of β-glucan-fatty acid esters.

Table 2
DS, IR band ratio of the BGFAs and average particle size of film forming emulsions.

Elementary and FTIR data			Average particle size	
Samples	DS	IR band ratio	Emulsions	d_{32} (μm)
LABG	2.08	1.33	AX-LABG	0.640 ± 0.031
MABG	2.17	1.34	AX-MABG	0.778 ± 0.039
PABG	2.04	1.31	AX-PABG	1.700 ± 0.392
SABG	2.03	1.35	AX-SABG	2.048 ± 0.208
OABG	2.09	1.28	AX-OABG	0.626 ± 0.064

Table 3
Moisture content of films at different% RH.

Film	Moisture content		
	50% RH	72% RH	98% RH
AX-BG	15.2 ± 0.4	17.7 ± 0.6	45.5 ± 0.5
AX-LABG	15.7 ± 0.4	18.8 ± 0.4	35.4 ± 0.6
AX-MABG	16.9 ± 0.1	18.9 ± 0.3	33.8 ± 0.8
AX-PABG	16.7 ± 0.3	19.0 ± 0.8	30.6 ± 0.7
AX-SABG	16.2 ± 0.9	18.9 ± 0.1	29.1 ± 0.7
AX-OABG	14.9 ± 0.5	16.0 ± 0.3	28.5 ± 0.6

low density polyethylene (LDPE) blended films reported that concentration of glycerol up to 18% improved the adhesion between polar and non-polar constituents whereas glycerol content up to 25% retained good functional properties in the composite films (Pushpadass, Bhandari, & Hanna, 2010). In our study, glycerol (20%) was used as both plasticizer and compatibilizer to improve the interfacial adhesion between polar AX and hydrophobic BGFAs. The thickness of films varied from 23 to 32 μm.

3.5. Water content of the films

Water absorption of the AX-BG and AX-BGFAs composite films were examined at different relative humidities (% RH) and the results were summarized in Table 3. At RH 50% and 72%, addition of BGFAs to AX produced no notable variation in the water content which may be attributed to the lower water absorption capacity of arabinoxylans (Sárossy et al., 2013). However, at RH 98% a significant decreasing tendency in the water content was observed for AX-BGFAs films suggested increased hydrophobicity played role in reducing water absorption. The water absorption of the AX-BGFAs films decreased as the chain length of the fatty acids increased and the lowest water content were observed for AX-SABG and AX-OABG films (29.1% and 28.5% respectively).

3.6. Structural properties

The film microstructures were determined by SEM to know the arrangements of different components in the dried films. Fig. 2 showed the SEM micrograms of cross sections of both AX-BG and AX-BGFAs films. The AX-BG film showed a smooth homogenous aspect with continuous surface in polymer matrix. Films with saturated BGFAs (AX-LABG, AX-MABG and AX-PABG) showed laminar structures which can be associated with the growth of molecular aggregation of fatty acids during film drying and final crystallization of fatty acids in matrix. The laminar structures were observed due to the water loss of laminar micelles that are formed above a determined concentration of esterified fatty acids in aqueous phase. The length of lipid layers were greater for AX-LABG film and decreased as the chain length increased, smallest lipid layers were observed for AX-SABG film. This suggested that the greater molecular mobility of shorter chain fatty acids was responsible for more effective growth of bi-layer self-association of molecule aggregates and creaming phenomenon (Fabra et al., 2009). Similar microstructures were found in earlier studies for sodium caseinate films with different saturated fatty acids (Fabra et al., 2009). For the AX-OABG film, the double bond in OA limited its self-association in aqueous medium, thus OABG seems finely distributed in the polymer matrix and a non-layer microstructure was observed.

3.7. WVP analysis

Addition of β-glucan to AX film had no effect on reducing the water vapor permeability; the higher WVP value was found due

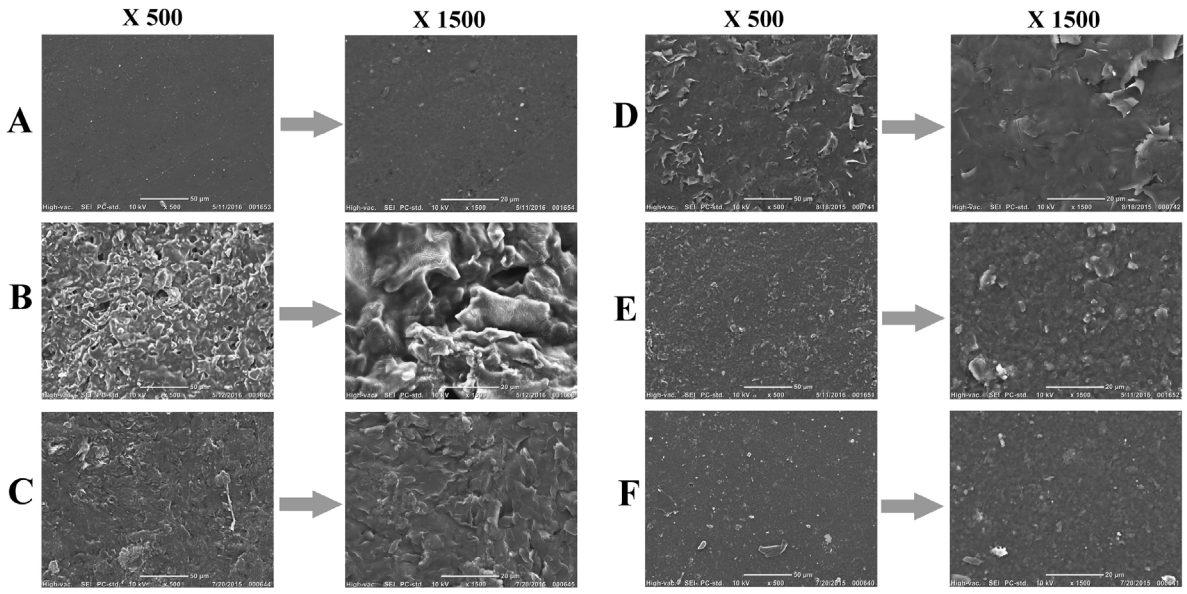

Fig. 2. SEM cross sectional images of AX-BG (A), AX-LABG (B), AX-MABG (C), AX-PAPG (D), AX-SABG (E) and AX-OABG (F) films at different magnifications.

Table 4
Water vapor transmission rate (WVTR), water vapor permeability (WVP), tensile strength (TS) and elongation at break (E%) of different films.

Film	WVTR ($g/m^2/24\,h$)	WVP ($g\,mm/KPa/m^2/24\,h$)	TS (MPa)	E (%)
AX	287.9 ± 25.3	23.1 ± 2.8	7.7 ± 0.4	6.9 ± 0.7
AX-BG	258.7 ± 14.8	20.7 ± 1.2	14.4 ± 2.8	5.7 ± 0.2
AX-LABG	52.7 ± 5.9	3.0 ± 0.3	5.7 ± 0.6	1.9 ± 0.6
AX-MABG	99.1 ± 10.5	6.5 ± 1.0	9.2 ± 1.6	2.9 ± 0.6
AX-PABG	93.5 ± 7.5	5.7 ± 0.5	8.7 ± 0.2	2.5 ± 0.4
AX-SABG	130.7 ± 16.7	6.8 ± 1.0	12.3 ± 0.8	2.4 ± 0.1
AX-OABG	158.9 ± 15.9	9.8 ± 1.0	7.9 ± 0.1	3.9 ± 0.1
LDPE[a]			9–17	500

[a] Briston (1988).

to higher water affinity of β-glucan and large numbers of binding sites to form H-bonds in presence of water (Sárossy et al., 2013). The measured WVP value for AX-BG film (60:40, w/w) was within the same range as previously found for rye arabinoxylans and β-glucan films (50:50) (Sárossy et al., 2013). As expected, addition of BGFAs to AX reduced the water vapor transmission because of the increase in film's hydrophobicity (Table 4). The improvement in water barrier properties due to addition of fatty acids to HMPC and protein based films were described in earlier studies (Fabra et al., 2009; Jiménez et al., 2010). Some authors reported that water barrier properties of films increased as the chain length of fatty acids and hydrophobicity increased (Fabra et al., 2009). However, our result indicated that micro-structural arrangements of films played a more relevant role controlling the water vapor transmission properties. Fig. 2 showed that AX-LABG film with laminar structures comprising greater successive layers contributed most effectively to reduce the water vapor transmission and improved the water barrier properties. Furthermore, a decrease in the water barrier effectiveness was observed when the layers got smaller (AX-SABG). This explained the poor water barrier properties of AX-SABG compared to AX-PABG and AX-MABG films despite of its greater hydrophobicity. The film containing AX-OABG had lowest water barrier efficiency than those formulated with saturated BGFAs films; this effect may be attributed to its high molecular volume associated with un-saturation and non-layer microstructure of the film (Fabra et al., 2009; Jiménez et al., 2010).

3.8. Mechanical properties

Tensile strength (TS) and elongation at break (E) are very important parameters related to the mechanical properties of films when they have been applied to a food product. Edible films must represent a good compromise between tensile strength and elongation and more specifically for edible coating; they have to be thin and tender in order to be imperceptible during eating. In our study, tensile strength of AX film was lower than previously reported values for rye and maize bran arabinoxylans (Péroval et al., 2002; Sárossy et al., 2013). This could be due to several factors such as: arabinoxylan composition and source, presence of polyphenols and 'associated lignins, plasticizing effect of glycerol, film preparation and storage (Rubilar et al., 2013; J. Wu, Wang, Li, Li, & Wang, 2009). However, addition of BG to AX film resulted in an increase in tensile strength by nearly 1.9 fold. Furthermore, the influence of fatty acids attached to BG on mechanical properties of AX was further investigated. The addition of BGFAs to AX caused reduction in tensile strength and elongation at break due to introduction of discontinuities in the film matrix. For AX and saturated BGFAs composite films, TS and E (%) decreased as the size of the lipid layers increased which can be associated with the greater mechanical resistance of smaller particles than big (Table 4). The AX-SABG film with smaller lipid layers produced a smaller decrease in mechanical resistance with respect to AX-BG film. The nearly equal tensile strength of AX-PABG and AX-MABG films could be attributed to their similar microstructures. However, the film containing AX-OABG despite of its non-layer microstructure produced low mechanical resistance. This behavior can be explained by the synergistic plasticizing effect of water and OA (Fabra et al., 2009; Fabra, Talens, & Chiralt, 2008), at intermediate RH (58%) the strong interactions between polar groups of OA and water might be responsible for reduction in the cohesive forces between polymer chains and increase in film flexibility compared to AX-saturated BGFAs films (Fabra et al., 2009). In comparison with synthetic film low density polyethylene (LDPE), AX and long chain BGFAs composite films exhibited similar tensile strengths, but they are less deformable.

3.9. Optical properties

The most important parameters related to optical properties which have impact on the appearance of the coated food products

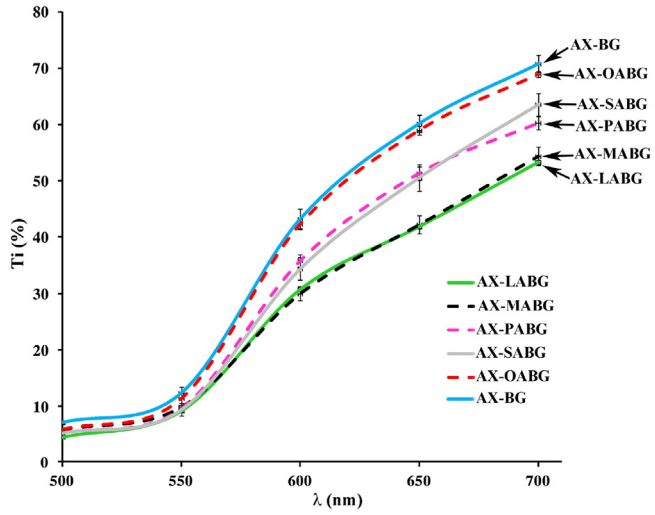

Fig. 3. Spectral distribution of internal transmittance of AX-BG and AX-BGFAs composite films.

are color and transparency (Hutchings, 1999). Higher Ti values correspond to greater film homogeneity and transparency whereas lower Ti values suggest the films are more opaque. The spectral distribution curves (Fig. 3) of Ti parameters showed the film with AX-OABG had no notably increase in opacity compared to AX-BG film. However, when saturated BGFAs were added to AX, the opacity increased as the size of the lipid aggregates increased in the matrix. The films with greater successive layers (AX-LABG and AX-MABG) provoked highly light dispersion, leading to more opaque matrices. The results suggest that AX-OABG film can potentially be used for coating surfaces where higher transparency is desirable. For some other applications where the product is required to be protected against light and related deteriorative reactions, films with lower transparency could be employed. The obtained Ti values were also well supported by microstructures analysis of the films using SEM.

All the films had slightly reddish-yellow appearance, as evident by higher b*, a* and lower WI values; this can be explained by the presence of phenolic compounds in AX matrix which might be responsible for light absorption and poor light transmission at lower wavelength (~500–570 nm) (Akhtar et al., 2010; Costa et al., 2015). Nevertheless, this causes no problem when films applied for particular product. The detail of WI and color values including L*, a* and b* were summarized in Supplementary Table S1.

3.10. Thermal stability

The thermo-gravimetric analysis (TGA) of the pure AX, AX-BG and AX-BGFAs films was employed to characterize their decomposition and thermal stability (Fig. 4). The incorporation of BG to AX-film did not influence the thermal stability, the weight loss of pure AX and AX-BG composite films started very slowly to a maximum of ~10% at around 133 °C which could be due to vaporization of absorbed and bound water (Mohammad, Razavi, Amini, & Zahedi, 2015). By further heating, AX and AX-BG films showed two stages of major thermal degradations ranges in 166–246 °C and 254–369 °C; probably corresponds to the loss of plasticizer (glycerol) and breakdown of polymer chains (cleavage of glycosidic bonds and side chains) to reasonably high mass volatiles in the first stage followed by complete degradation of macromolecules in the second stage (Iqbal, Akbar, Hussain, Saghir, & Sher, 2011; Mohammad et al., 2015). In contrast, all the AX-BGFAs composite films exhibited multistep decomposition curves with similar degradation patterns, the first stage of the thermo-grams displayed a small peak at around 49.9-89.9 °C revealing free water loss (Mohammad et al., 2015); followed by a weight loss between 120 °C and 200 °C likely to be associated with volatilization of bound water and plasticizer (glycerol) (Mohammad et al., 2015); ending with two abrupt degradation peaks in the temperature range of 209–300 °C and 306–417 °C related to the polysaccharide scission and complete decomposition. It could be concluded that esterification of BG shifted the degradation temperature of AX-BGFAs composite films towards higher values (by about 48 °C) suggesting an increase in the thermal stability compared to native AX and AX-BG films. The result was consistent with the earlier reported

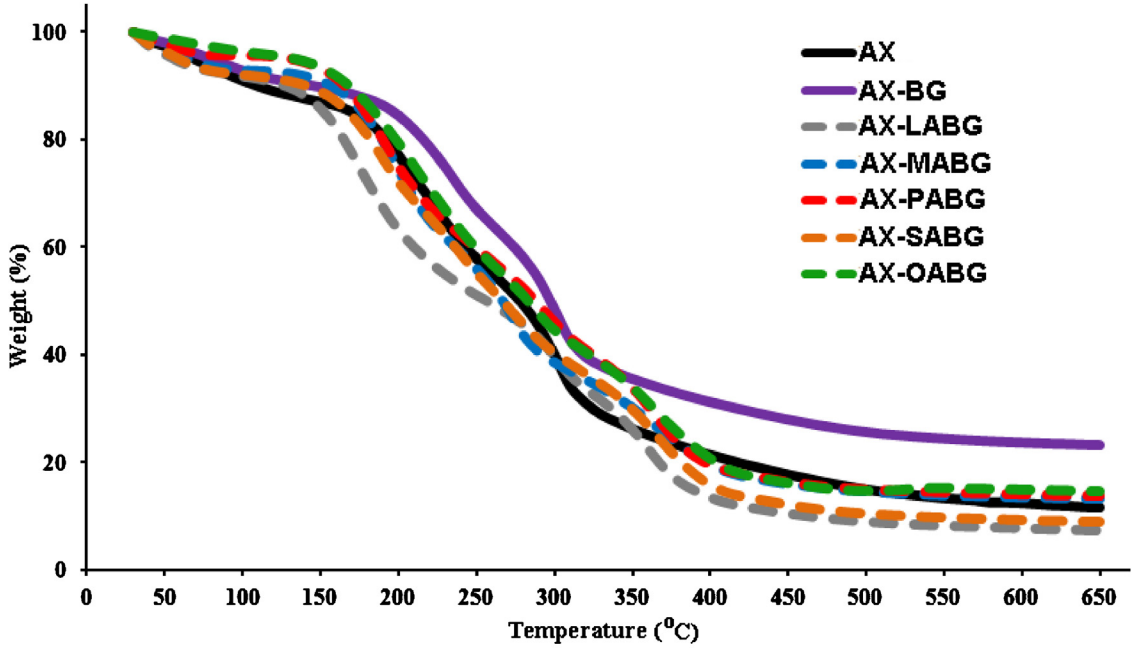

Fig. 4. TGA curves of pure AX, AX-BG and AX-BGFAs composite films.

observations that esterification of OH groups in polysaccharides were beneficial for the improvement in thermal stability (Buchanan et al., 2003; Winkler, Vorwerg, & Rihm, 2014). At the end of the analysis (650 °C), it was noted that AX-BG film had higher residual weight than pure AX and AX-BGFAs composite films which was probably due to higher salt content in the initial material (Reddy & Rhim, 2014). Nonetheless, previous studies have shown that the high value of residual rate may imply the good flame retardance of the material (Jiang, Zhao, & Hou, 2016).

4. Conclusions

The properties of edible AX based films were greatly affected by incorporation of fatty acid esterified β-glucans. All AX-BGFAs composite films exhibited similar thermal degradation patterns and found to be thermally more stable than AX and AX-BG films. Further study revealed that microstructures of films played relevant role in controlling the water vapor permeability, optical and mechanical properties. Saturated BGFAs with shorter chain length were self-associated as laminar structures in the dried films. The laminar structures greatly limited the WVP, at the same time resulted in more opaque films. On contrary, AX-SABG and AX-OABG films with lower opacity were less effective in improvement in water vapor permeability due to lack of multilayer film microstructures. Furthermore, laminar structures in the films resulted in reduction in tensile strength and stretchability. Incorporation of SABG to AX lead to films with best properties, improved thermal stability, reduced the WVP to about 67% and produced no significant reduction in mechanical strength compared to native AX-BG film. To our knowledge, this represents the first report of compatible blends formed by combining the fatty acid ester derivatives of BG with AX. The ability to easily prepare these β-glucan-fatty acid esters and to incorporate them into AX offers intriguing possibilities of preparing novel composites. However, further studies are needed to investigate potential performance improvement for industrialized use of the films for food products.

Acknowledgements

Authors thank Executive Director, NABI for encouragement and support. The authors thank National Agri-Food Biotechnology Institute (NABI) and Department of Biotechnology (DBT), Govt. of India for the financial support. Authors would also like to thank DBT-e-Libray Consortium (DELCON) for providing acess to online resources. We are thankful to Sh. Jagdeep Singh for technical assistance. Usman Ali is thankful to NABI and DBT for research fellowship.

Appendix A. Supplementary data

Supplementary data associated with this article can be found, in the online version, at http://dx.doi.org/10.1016/j.carbpol.2016.12.036.

References

AOAC. (2000). *β-D-Glucan in barley and oats, streamlined enzymatic method*. Washington, DC: Association of Official Analytical Chemist.

ASTM. (2002). Standard test method for tensile properties of thin plastic sheeting. In *Method ASTM D 882*. Philadelphia, PA: American Society for Testing and Materials.

ASTM. (2005). Standard test methods for water vapor transmission of materials. In *Method E96/E96-05*. Philadelphia, PA: American Society for Testing and Materials.

Ahmad, A., Anjum, F. M., Zahoor, T., Nawaz, H., & Ahmed, Z. (2010). Extraction and characterization of β-d-glucan from oat for industrial utilization. *International Journal of Biological Macromolecules*, *46*, 304–309.

Akhtar, M. J., Jacquot, M., Arab-Tehrany, E., Gaiani, C., Linder, M., & Desobry, S. (2010). Control of salmon oil photo-oxidation during storage in HPMC packaging film: Influence of film colour. *Food Chemistry*, *120*, 395–401.

Arnon, H., Granit, R., Porat, R., & Poverenov, E. (2015). Development of polysaccharides-based edible coatings for citrus fruits: A layer-by-layer approach. *Food Chemistry*, *166*, 465–472.

Briston, J. H. (1988). *Plastic film* (3rd ed.). New York, NY: John Wiley & Sons.

Buchanan, C. M., Buchanan, N. L., Debenham, J. S., Gatenholm, P., Jacobsson, M., Shelton, M. C., et al. (2003). Preparation and characterization of arabinoxylan esters and arabinoxylan ester/cellulose ester polymer blends. *Carbohydrate Polymers*, *52*, 345–357.

Costa, M. J., Cerqueira, M. A., Ruiz, H. A., Fougnies, C., Richel, A., Vicente, A. A., et al. (2015). Use of wheat bran arabinoxylans in chitosan-based films: Effect on physicochemical properties. *Industrial Crops and Products*, *66*, 305–311.

Dubois, M., Gilles, K. A., Hamilton, J. K., Rebers, P. A., & Smith, F. (1956). Colorimetric method for determination of sugars and related substances. *Analytical Chemistry*, *28*, 350–356.

Ebringerova, A., Hromadkova, Z., & Heinze, T. (2005). Hemicellulose. *Advances in Polymer Science*, *186*, 1–67.

Fabra, M. J., Talens, P., & Chiralt, A. (2008). Tensile properties and water vapor permeability of sodium caseinate films containing oleic acid-beeswax mixtures. *Journal of Food Engineering*, *85*, 393–400.

Fabra, M. J., Jiménez, A., Atarés, L., Talens, P., & Chiralt, A. (2009). Effect of fatty acids and beeswax addition on properties of sodium caseinate dispersions and films. *Biomacromolecules*, *10*, 1500–1507.

Fox, A., Morgan, S. L., & Gilbart, L. (1989). Preparation of alditol acetate and their analysis by gas chromatography and mass spectrometry. In C. J. Bierman, & G. McGinnis (Eds.), *Analysis of Carbohydrate by GLC and MS* (pp. 88–116). Boca Raton: CRC Press.

Freire, C. S. R., Silvestre, A. J. D., Neto, C. P., & Rocha, R. M. A. (2005). An efficient method for determination of the degree of substitution of cellulose esters of long chain aliphatic acids. *Cellulose*, *12*, 449–458.

Gröndahl, M., & Gatenholm, P. (2007). Oxygen barrier films based on xylans isolated from biomass. In S. A. Dimitris (Ed.), *Materials, chemicals, and energy from forest biomass* (pp. 137–152). Washington, DC: American Chemical Society.

Gruppen, H., Hamer, R. J., & Voragen, A. G. J. (1992). Water-unextractable cell wall material from wheat flour. 1. Extraction of polymers with alkali. *Journal of Cereal Science*, *16*, 41–51.

Höije, A., Sternemalm, E., Heikkinen, S., Tenkanen, M., & Gatenholm, P. (2008). Material properties of films from enzymatically tailored arabinoxylan. *Biomacromoleculaes*, *9*, 2042–2047.

Hutchings, J. B. (1999). *Food color and appearance* (2nd ed.). Gaithersburg, MD: Chapman and Hall Food Science Book, Aspen Publication.

Iqbal, M. S., Akbar, J., Hussain, M. A., Saghir, S., & Sher, M. (2011). Evaluation of hot-water extracted arabinoxylans from ispaghula seeds as drug carriers. *Carbohydrate Polymers*, *83*, 1218–1225.

Jiang, X., Zhao, Y., & Hou, L. (2016). The effect of glycerol on properties of chitosan/poly (vinyl alcohol) films with AlCl 3·6H 2 O aqueous solution as the solvent for chitosan. *Carbohydrate Polymers*, *135*, 191–198.

Jiménez, A., Fabra, M. J., Talens, P., & Chiralt, A. (2010). Effect of lipid self-association on the microstructure and physical properties of hydroxypropyl-methylcellulose edible films containing fatty acids. *Carbohydrate Polymers*, *82*, 585–593.

Jimenez, A., Fabra, M. J., Talens, P., & Chiralt, A. (2012). Influence of hydroxypropylmethylcellulose addition and homogenization conditions on properties and ageing of corn starch based films. *Carbohydrate Polymers*, *89*, 676–686.

Knutson, C. A., & Jeanes, A. (1968). A new modification of the carbazole analysis: Application to heteropolysaccharides. *Analytical Biochemistry*, *24*, 470–481.

Mikkonen, K. S., Heikkinen, S., Soovre, A., Peura, M., Serimaa, R., Talja, R. A., et al. (2009). Films from oat spelt arabinoxylan plasticized with glycerol and sorbitol. *Journal of Applied Polymer Science*, *114*, 457–466.

Mohajer, S., Rezaei, M., & Hosseini, S. F. (2016). Physico-chemical and microstructural properties of fish gelatin/agar bio-based blend films. *Carbohydrate Polymers*, *157*, 784–793.

Mohammad, S., Razavi, A., Amini, A. M., & Zahedi, Y. (2015). Characterisation of a new biodegradable edible film based on sage seed gum: In fl uence of plasticiser type and concentration. *Food Hydrocolloids*, *43*, 290–298.

Mukherjee, S., & Ghosh, M. (2016). Studies on performance evaluation of a green plasticizer made by enzymatic esterification of furfuryl alcohol and castor oil fatty acid. *Carbohydrate Polymers*, http://dx.doi.org/10.1016/j.carbpol.2016.10.075

Otoni, C. G., Avena-Bustillos, R. J., Olsen, C. W., Bilbao-Sáinz, C., & McHugh, T. H. (2016). Mechanical and water barrier properties of isolated soy protein composite edible films as affected by carvacrol and cinnamaldehyde micro and nanoemulsions. *Food Hydrocolloids*, *57*, 72–79.

Péroval, C., Debeaufort, F., Despré, D., & Voilley, A. (2002). Edible arabinoxylan-based films. 1. Effects of lipid type on water vapor permeability, film structure, and other physical characteristics. *Journal of Agricultural and Food Chemistry*, *50*, 3977–3983.

Phan The, D., Debeaufort, F., Peroval, C., Despre, D., Courthaudon, J. L., & Voilley, A. (2002). Arabinoxylan-lipid-based edible films and coatings. 3. Influence of drying temperature on film structure and functional properties. *Journal of Agricultural and Food Chemistry*, *50*, 2423–2428.

Phan The, D., Debeaufort, F., Voilley, A., & Luu, D. (2009). Influence of hydrocolloid nature on the structure and functional properties of emulsified edible films. *Food Hydrocolloids*, *23*, 691–699.
Pushpadass, H. A., Bhandari, P., & Hanna, M. A. (2010). Effects of LDPE and glycerol contents and compounding on the microstructure and properties of starch composite films. *Carbohydrate Polymers*, *82*, 1082–1089.
Ratanakamnuan, U., Manorom, W., & Inthasai, P. (2013). Preparation of biodegradable film from esterified corn husk cellulose. *Advanced Materials Research*, *701*, 229–233.
Razzaq, H. A. A., Pezzuto, M., Santagata, G., Silvestre, C., Cimmino, S., Larsen, N., et al. (2016). Barley β-glucan-protein based bioplastic film with enhanced physicochemical properties for packaging. *Food Hydrocolloids*, *58*, 276–283.
Reddy, J. P., & Rhim, J. (2014). Characterization of bionanocomposite films prepared with agar and paper-mulberry pulp nanocellulose. *Carbohydrate Polymers*, *110*, 480–488.
Rubilar, J. F., Cruz, R. M. S., Silva, H. D., Vicente, A. A., Khmelinskii, I., & Vieira, M. C. (2013). Physico-mechanical properties of chitosan films with carvacrol and grape seed extract. *Journal of Food Engineering*, *115*, 466–474.
Ruiz, H. A., Cerqueira, M. A., Silva, H. D., Rodríguez-Jasso, R. M., Vicente, A. A., & Teixeira, J. A. (2013). Biorefinery valorization of autohydrolysis wheat straw hemicellulose to be applied in a polymer-blend film. *Carbohydrate Polymers*, *92*, 2154–2162.
Sárossy, Z., Tenkanen, M., Pitkänen, L., Bjerre, A. B., & Plackett, D. (2013). Extraction and chemical characterization of rye arabinoxylan and the effect of β-glucan on the mechanical and barrier properties of cast arabinoxylan films. *Food Hydrocolloids*, *30*, 206–216.
Singleton, V. L., Orthofer, R., & Lamuela-Raventos, R. M. (1998). Analysis of total phenols and other oxidation substrates and antioxidants by means of folin-ciocalteu reagent. *Methods in Enzymology*, *299*, 152–178.
Subba Rao, M. V. S. S. T., & Muralikrishna, G. (2006). Hemicelluloses of ragi (Finger millet, Eleusine coracana, indaf-15): Isolation and purification of an alkali-extractable arabinoxylan from native and malted hemicellulose B. *Journal of Agricultural and Food Chemistry*, *54*, 2342–2349.
Tejinder, S. (2003). Preparation and characterization of films using barley and oat β-glucan extracts. *Cereal Chemistry*, *80*, 728–731.
Vaca-Garcia, B. M. E. (2001). Determination of the degree of substitution (DS) of mixed cellulose esters by elemental analysis. *Cellulose*, *8*, 225–231.
Whistler, R. L. (1945). Preparation and properties of starch ester. *Advance in Carbohydrate Chemistry*, *1*, 279–307.
Winkler, H., Vorwerg, W., & Wetzel, H. (2013). Synthesis and properties of fatty acid starch esters. *Carbohydrate Polymers*, *98*, 208–216.
Winkler, H., Vorwerg, W., & Rihm, R. (2014). Thermal and mechanical properties of fatty acid starch esters. *Carbohydrate Polymers*, *102*, 941–949.
Wu, R., Wang, X., Li, F., Li, H., & Wang, Y. (2009). Green composite films prepared from cellulose: Starch and lignin in room-temperature ionic liquid. *Bioresource Technology*, *100*, 2569–2574.
Xu, Y., Miladinov, V., & Hanna, M. A. (2004). Synthesis and characterization of starch acetates with high substitution. *Cereal Chemistry*, *81*, 735–740.
Ying, R., Saulnier, L., Bouchet, B., Barron, C., Ji, S., & Rondeau-Mouro, C. (2015). Multiscale characterization of arabinoxylan and β-glucan composite films. *Carbohydrate Polymers*, *122*, 248–254.
Zhang, P., & Whistler, R. L. (2004). Mechanical properties and water vapor permeability of thin film from corn hull arabinoxylan. *Journal of Applied Polymer Science*, *93*, 2896–2902.
Zhang, Y., Pitkänen, L., Douglade, J., Tenkanen, M., Remond, C., & Joly, C. (2011). Wheat bran arabinoxylans: Chemical structure and film properties of three isolated fractions. *Carbohydrate Polymers*, *86*, 852–859.
Zhu, F., Du, B., & Xu, B. (2016). A critical review on production and industrial applications of beta-glucans. *Food Hydrocolloids*, *52*, 275–288.